

Anisotropy in magnetic and transport properties of LaTSb_3 ($T=\text{Cr, V}$)

D. D. Jackson,* M. Torelli, and Z. Fisk

National High Magnetic Field Laboratory, Tallahassee, Florida 32310

(Received 23 April 2001; published 4 December 2001)

We report measurements of anisotropy in magnetic susceptibility, magnetization, and electrical resistivity using single crystals of LaTSb_3 ($T=\text{Cr, V}$). LaTSb_3 is a quasi-two-dimensional system with an orthorhombic crystal structure (space group $Pbcm$), possessing a rich phase diagram with a ferromagnetic transition at $T_C = 132$ K due to the ordering of the Cr ions. In order to investigate LaTSb_3 , magnetic susceptibility and magnetization for fields up to 55 kG and in the temperature range of 2–350 K have been measured with the field aligned to the three principle axes. The electrical resistivity of LaCrSb_3 has been measured for currents parallel to the a , b , and c axes in the temperature range 5–295 K, as well as magnetoresistances at 20 k and 60 kG along the b axis. Isostructural LaVSb_3 is found have no transitions in either the magnetization or the resistivity; therefore, it is presented as a nonmagnetic counterpart. Just below T_C , the easy axis is found to be within the b - c plane in the direction of the magnetic field. As the system is further cooled, there is a crossover from quasi-two-dimensional (2D) to 3D anisotropy below a characteristic temperature T^* , and the easy axis of magnetization becomes oriented along the b axis. Furthermore, it is found that T^* decreases linearly as the magnetic field is increased, and is suppressed with a field $H > 3.7$ kG. A high-temperature antiferromagnetic transition is found at $T_N = 98$ K. The value of T_N is found to be independent of the applied magnetic field up to $H = 0.25$ kG, at which point this antiferromagnetic phase is suppressed.

DOI: 10.1103/PhysRevB.65.014421

PACS number(s): 75.30.Gw, 75.30.Kz, 75.50.Cc, 72.15.-v

I. INTRODUCTION

LaTSb_3 ($T=\text{Cr, V}$) has recently been of interest in the literature due to its quasi-two-dimensional crystal structure and rich phase diagram.^{1–6} Polycrystalline measurements of LaCrSb_3 have shown that it undergoes an itinerant ferromagnetic (FM) transition due to the Cr ions, but the precise transition temperature is still in question. Replacing Cr with V eliminates the $3d$ moment, and the magnetic ordering vanishes.

While the general trends observed in LaTSb_3 show similar behaviors throughout the literature, some of the specific quantitative details are in disagreement. The crystal structure,^{1,2} magnetization, and electrical resistivity^{3–5} have been investigated on polycrystalline samples. In these studies, a ferromagnetic transition in LaCrSb_3 was observed at $T_C = 125$ K (Refs. 3 and 6) or $T_C = 142$ K,^{4,5} with the difference apparently arising from the sample growth procedures. The single-crystal work was limited to a single study by Raju *et al.*,⁶ in which the electrical resistivity along only the c axis was investigated. Their work also included neutron-diffraction measurements on polycrystalline LaCrSb_3 , in which they found Cr moments aligned along the b axis, as well as band-structure calculations which predicted the electrical resistivity to be lowest (highest) along the c axis (a axis). Although crystal-structure and band-structure calculations suggested that anisotropy will play a crucial role in the physics of this system, to our knowledge this is the first study in which single crystals have been grown whose morphology allow for a systematic study of the magnetization and electrical resistivity properties along the three principal axes.

LaCrSb_3 is only one member in the family of compounds, $R\text{CrSb}_3$ ($R=\text{La-Nd, Sm, Gd}$).⁷ An in-depth investigation into LaCrSb_3 has been undertaken because, in this compound, all

of the magnetic transitions are due to the $3d$ electrons of Cr, and so this provides a baseline for an understanding of the remaining light rare earth compounds. While it is common to find an antiferromagnetic (AFM) phase in Cr-based alloys,⁸ LaCrSb_3 is found to have a rare FM transition at $T_C = 132$ K for all magnetic fields investigated. A surprising property of this system is the presence of an apparent AFM transition whose Néel temperature ($T_N = 98$ K) is less than the Curie temperature ($T_C = 132$ K), and is suppressed with a rather small magnetic field (250 G). While two magnetic transitions have been observed for d -electron systems, these tend to be found in mixed-valent materials such as $\text{La}_{1-x}\text{Ca}_x\text{MnO}_3$,^{9–11} in which the interactions between neighboring Mn^{3+} ions are FM (positive coupling), neighboring Mn^{4+} ions are AFM (negative coupling), and Mn^{3+} and Mn^{4+} neighbors are found to couple ferromagnetically (positive coupling). Two AFM transitions have been observed in $\text{Ca}_3\text{Ru}_2\text{O}_7$,¹² which undergoes a spin reorientation within the AFM phase, but the coupling between the Ru ions are always found to be AFM (negative). In contrast, LaCrSb_3 is a pure compound in which the coupling between neighboring magnetic ions is found to change from positive (FM) to negative (AFM). In addition, there is also high magnetic anisotropy within the quasi-two-dimensional (2D) plane, which leads to a surprisingly rich phase diagram. These newly discovered properties can only be investigated with high quality single crystals.

LaCrSb_3 crystallizes in an orthorhombic structure (space group $Pbcm$)¹ with the lattice constants $a = 13.29(1)$ Å, $b = 6.21(1)$ Å, $c = 6.11(9)$ Å. The lattice constants for LaVSb_3 are $a = 13.36(9)$ Å, $b = 6.25(6)$ Å, and $c = 6.05(9)$ Å. The crystal structure consists of two distinct layers of Cr and Sb perpendicular to the a axis which are separated by rare-earth ions (Fig. 1). The first of these layers consists of chains of Cr atoms extending along the c direc-

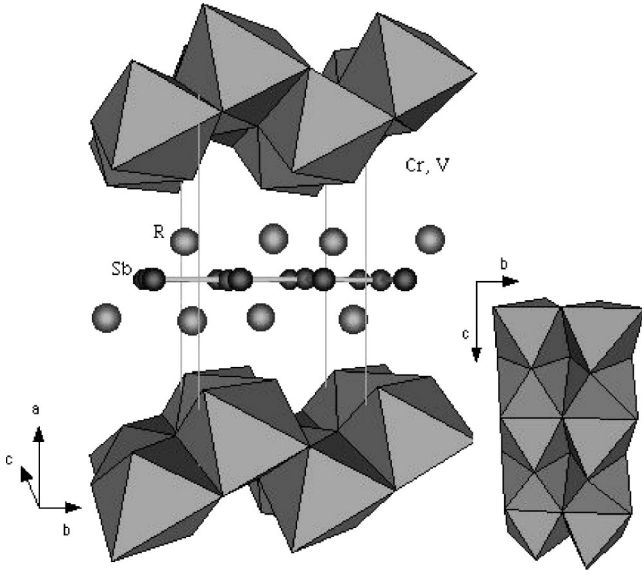


FIG. 1. LaTSb_3 crystal structure. The Sb octahedra surround the transition-metal ion, while the rare-earth ions lie above and below the Sb square plane. The octahedra are edge sharing along the b axis and face sharing along the c axis, as can be seen in the inset.

tion, with Sb atoms forming face-sharing (edge-sharing) octahedra along the c axis (b axis). The second layer consists of nearly square sheets of Sb atoms in the b - c plane. The rare-earth ions lie in a checkerboard-type pattern which alternates above and below the Sb plane. This quasi-2D crystal structure suggests that anisotropy may play a crucial role in understanding its properties.

II. EXPERIMENTAL TECHNIQUE

Single crystals of LaTSb_3 were prepared from ingots of the elements [La from Ames Laboratory; Cr (99.996%), V (99.5%), and Sb (99.99%) from Alfa Aesar]. The constituents La:(Cr,V):Sb were mixed in the ratio 4:3:13 in alumina crucibles, heated to 1180°C in a controlled atmosphere, and then cooled at a rate of $10^\circ/\text{h}$ to 750°C , at which point the flux was spun off using a centrifuge. The resulting crystals were rectangular planes with a thin face parallel to the a axis and the longest side parallel to the c axis, and had typical dimensions of $a:b:c=0.3:0.88:1.4$ mm. All measurements were taken on as grown samples. The lattice parameters were determined using a commercial Scintag x-ray diffractometer (Si standard) and a least-squares fit to a minimum of 20 peaks. Magnetization and magnetic susceptibility measurements were taken with a commercial superconducting quantum interference device (SQUID) magnetometer (Quantum Design MPMSR2) in the temperature range 2–350 K and $-55\text{ kG} \leq H \leq 55\text{ kG}$. Resistivity measurements were performed using a standard four-probe technique in the temperature range 5–295 K and in a magnetic field up to 60 kG.

III. RESULTS

A. Magnetization

The field-cooled magnetization as a function of temperature with an applied field of 1 kG for LaCrSb_3 is shown in

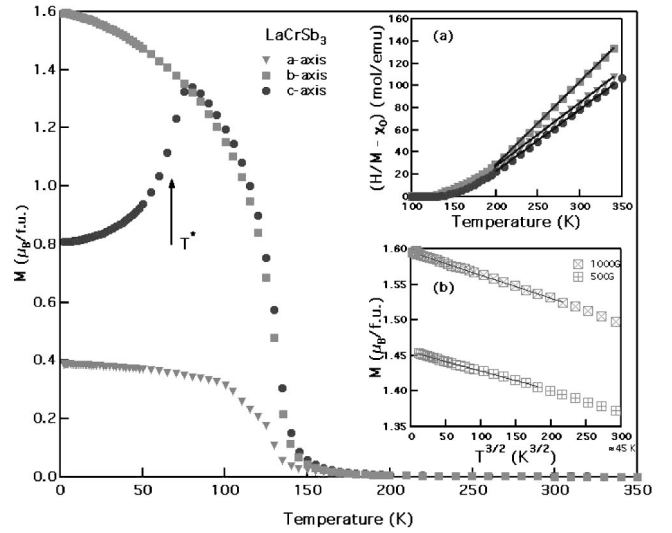


FIG. 2. Field-cooled magnetization vs temperature of all three crystallographic orientations of LaCrSb_3 with $T_C=132\text{ K}$ and $T^*=68\text{ K}$ seen along the c axis. The inset (a) shows the inverse susceptibility as a function of temperature, and (b) shows that the magnetization along the b axis increases as $T^{3/2}$.

Fig. 2. The FM transition at $T_C=132\text{ K}$ is clearly observable, as well as a feature in which the magnetic anisotropy is evident along all three crystallographic directions below $T^*=68\text{ K}$. Figure 3 shows the magnetic susceptibility of isostructural LaVSb_3 . In contrast to LaCrSb_3 , this material is nonmagnetic, and has minimal anisotropy. The susceptibility of LaVSb_3 is relatively temperature independent and very small, just above the resolution of the SQUID, and its positive value is expected for temperature-independent Pauli paramagnetism due to conduction electrons. The decrease in the noise of M_c above 150 K is due to an increase in the applied magnetic field in order to increase the signal response. Below approximately 30 K, the effects of a small number of impurities can be seen by the Curie tail in the magnetization. A comparison of the magnetization of the two isostructural compounds clearly shows that the magnetic behavior is due to the transition metal.

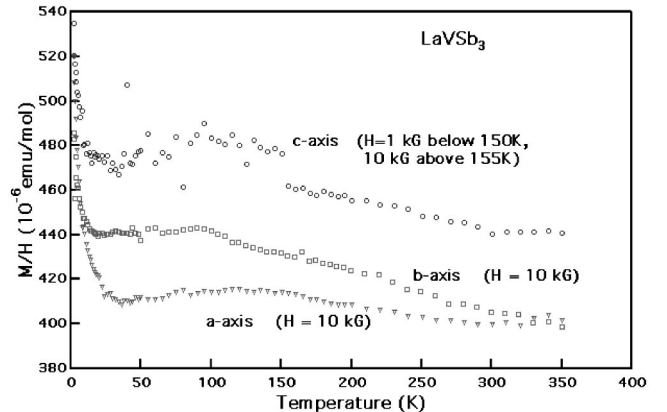


FIG. 3. Susceptibility vs temperature for LaVSb_3 . The very small and almost temperature-independent susceptibility makes this a nonmagnetic counterpart to LaCrSb_3 .

TABLE I. High-temperature Curie-Weiss data for LaCrSb₃. The error in χ_0 is 10%. The saturation values σ are found from M ($H = 55$ kG) at $T = 5$ K.

Axis	χ_0 (10^{-3} emu/mol)	μ_{eff} (μ_B /f.u.)	θ (K)	σ (μ_B /f.u.)
<i>a</i>	-2.05	3.79 ± 0.28	153 ± 20	1.31
<i>b</i>	-1.48	3.35 ± 0.27	163 ± 22	1.69
<i>c</i>	-2.15	3.87 ± 0.14	161 ± 9	1.74

Defining the susceptibility as $\chi = M/H$, the data for $T > 200$ K can be fit to a modified Curie-Weiss law, $\chi = \chi_0 + C/(T - \theta)$. The results for Curie-Weiss fit are seen in Fig. 2(a), and the parameters are listed in Table I. To simplify the analysis, a polycrystalline average of the susceptibility was used to determine an effective moment of $\mu_{eff} = 3.68\mu_B$ /f.u. One can then compare this experimental result with mean-field theory for Cr³⁺ ($S = 3/2$), which predicts $\mu_{eff} = 3.87\mu_B$.

Although this interpretation is enticing, it has become favorable in the literature to discuss LaCrSb₃ in terms of an itinerant FM system. There are several reasons for this. First, one notes that a very large and negative temperature-independent susceptibility χ_0 is found which does not seem to be physical. While a negative term may be expected, it can be calculated by summing up the individual diamagnetic contributions from each ion to be approximately -1×10^{-4} emu/mol,¹³ which is an order of magnitude smaller than what is observed. A nonphysical result such as this is often an indication that the Curie-Weiss law is not obeyed. Second, as will be shown shortly, the system is metallic, while the previous analysis should only hold for local-moment (nonmetallic) systems. Further evidence of itinerant behavior is a noninteger saturation moment (see Table I) and the loss of an esr signal above T_C .¹⁴

Figure 2 shows the field-cooled magnetization collected with an applied field of 1 kG. Evidence of the FM transition can be found as the magnetization increases along the three crystallographic orientations at $T_C = 132$ K. The Curie temperature was determined by the location of the peak in a plot of $-dM/dT$, which was consistent with the value determined from an Arrott plot. Just below T_C , both the *b* and *c* axis magnetizations lie on top of each other, while the *a* axis increases at a much slower rate. This result is consistent with the quasi-2D nature of the crystal structure.

The full anisotropy of the system becomes evident as the temperature is further reduced, and the *c* axis moment drops to $0.8\mu_B$ /f.u. One can define a characteristic temperature T^* , which is determined by the location of the peak of dM_c/dT at a constant field, below which the system is anisotropic along all three directions. Just below the Curie temperature, the easy axis of the magnetization is within the *b-c* plane, and oriented in the direction of the applied field. But as the temperature is lowered below T^* , the *b* axis becomes the easy axis of magnetization, and continues to rise as $T^{3/2}$ due to spin waves, as predicted by Stoner theory for itinerant FM [see Fig. 2(b)]. This result is in agreement with the polycrystalline neutron scattering data.⁶ The value of T^* depends

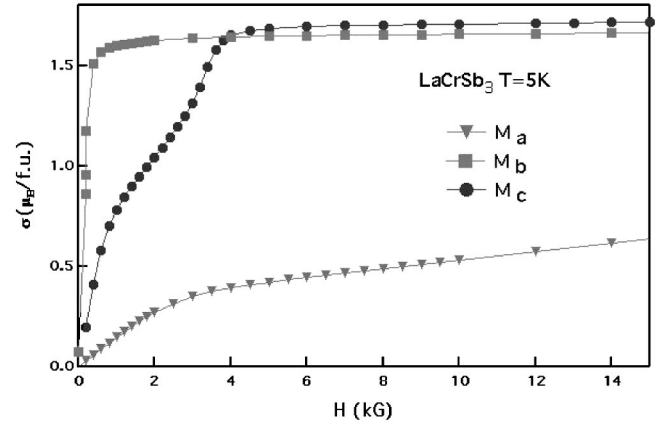


FIG. 4. Magnetization vs magnetic field for LaCrSb₃ at $T = 5$ K. The lines are a guide to the eye.

upon the applied field, and is found to be linearly depressed as the magnetic field was increased.

The magnetization as a function of field at 5 K is shown in Fig. 4. The magnetization along the *b* axis, the easy axis, saturates almost immediately as a step like function to $\sigma_b = 1.69\mu_B$ /f.u. A bump in the magnetization along the *c* axis found at $H = 3$ kG, which is associated with the downturn of M_c seen in Fig. 2 (recall that T^* was found to be field dependent). The *c* axis magnetization then saturates to approximately the same value as σ_b . The magnetization along the *a* axis behaves very differently from the previous two, and continues to increase linearly up to the maximum measured field of 55 kG. A quick review of the crystal structure (Fig. 1) will show that these results make qualitative sense in the fact that, within the *b-c* plane, the magnetization is found to be similar, but along the out-of-plane axis (*a* axis) the magnetization is unique. The saturation values at 55 kG for all three axes are listed in Table I. The discrepancy between M_b and M_c is most likely due to the slight misalignment of the sample within the applied magnetic field. Hysteresis is negligible for all three orientations.

The behavior of M_c along the Cr chains can be investigated with several constant field magnetization curves. Figures 5(a) and 5(b) show the data for various magnetic fields oriented along the *c* and *b* axes, respectively. Note that, for $H > 3.7$ kG, both the *b* and *c* axes have similar behaviors, and saturate to approximately $\sigma = 1.6\mu_B$ /f.u. This implies that the magnetic anisotropy within the *b-c* plane is less than 3.71 kG. The inset of Fig. 5(a) shows the behavior of T^* at various magnetic fields, which is the temperature below which the full anisotropy of the system is evident due to an alignment of the spins along the *b* axis. T^* is found to decrease linearly with the field, as seen in the inset to Fig. 5(a), and can be fit to the equation

$$T^*/94 \text{ K} = 1 - H^*/3.71 \text{ kG}. \quad (1)$$

A downturn in the magnetization was previously observed with polycrystalline samples,^{4,5} but to our knowledge this is the first investigation of its anisotropic behavior.

Figure 6 shows a recently discovered result as the applied field is lowered below 250 G, which is the presence of a

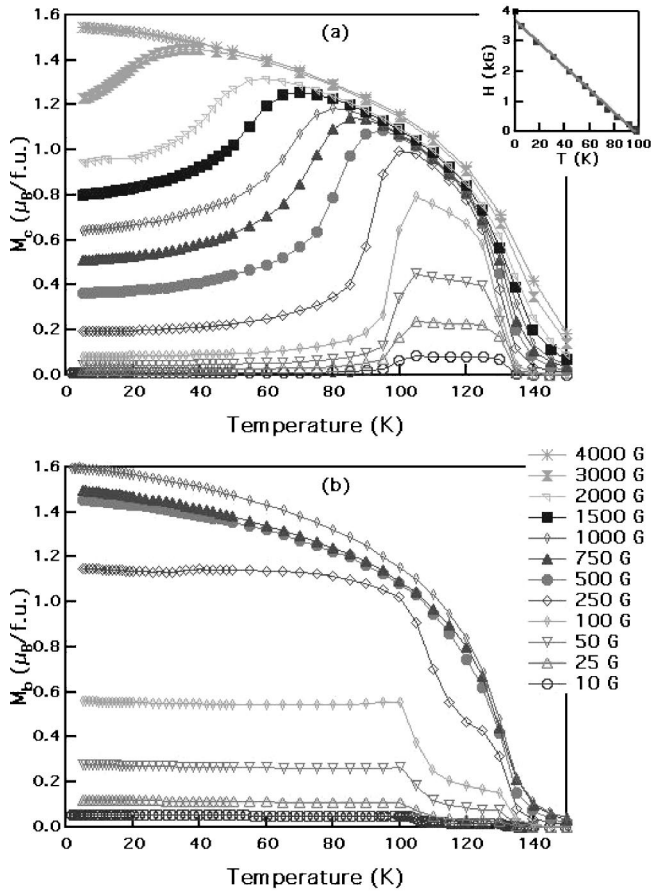


FIG. 5. (a) *c*-axis magnetization curves below T_C at various magnetic fields. For each field below 3.7 kG, there is a corresponding downturn at T^* defined by the peak in dM/dT . The inset shows that T^* decreases linearly with field. (b) *b*-axis magnetization curves show the presence of the AFM state, but above 250 G the *b* axis remains FM.

high-temperature antiferromagnetic state. The magnetization of all three axes is shown with an applied field of approximately 10 G. At $T_N = 98$ K the magnetization along the *c* axis has a sharp drop, while M_a and M_b remain flat and relatively temperature independent as the temperature is lowered. This is an indication of an AFM transition with the easy axis oriented along the Cr chains (the *c* axis).¹⁵ The insets to Fig. 6 show dM/dT along both the *b* and *c* axes, which indicate that this AFM transition is observed along both axes, and is field independent up to 250 G. Above this field, the decrease of M_c is not as sharp (the peak in dM_c/dT is reduced), and M_b continues to rise as the temperature is lowered, so that no peak in dM_b/dT is observed. This AFM phase has not been observed in magnetic measurements of polycrystalline samples. Furthermore, neutron-diffraction⁶ and thermal expansion³ measurements do not show any evidence of a structural transition at this temperature, but single-crystal neutron-diffraction measurements do show evidence for this transition.¹⁶

B. Electrical resistivity

Figure 7 shows the electrical resistivity for LaCrSb₃. The anisotropy of the system is clearly evident with the resistivity

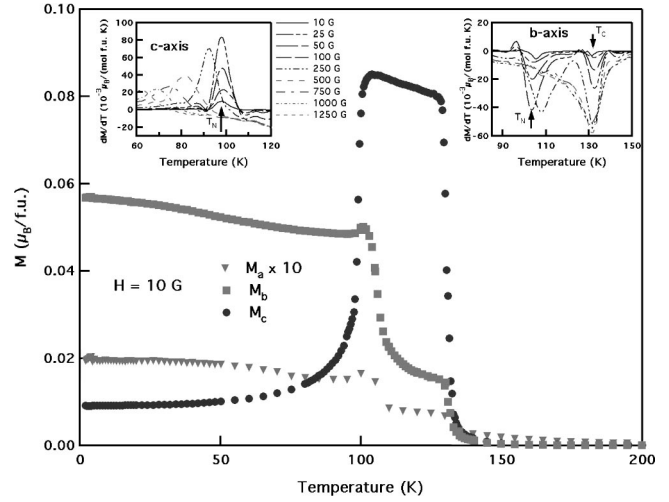


FIG. 6. $H = 10$ G field-cooled magnetization of LaCrSb₃. The FM transition is at $T_C = 132$ K, and the AFM transition is at $T_N = 98$ K. M_a is multiplied by a factor of 10 so that it can be seen to exhibit similar behavior to M_b . The inset shows dM/dT along both the *b* and *c* axes to show the behavior of the magnetization near T_N at various fields.

along the Cr chains of $\rho_c = 169 \mu\Omega$ cm, perpendicular to the chains $\rho_b = 483 \mu\Omega$ cm, and the out-of-plane resistivity is $\rho_a = 990 \mu\Omega$ cm. The values of the in-plane resistivity, as well as their positive slope throughout the temperature range investigated, indicate that these axes are both metallic. The out-of-plane resistivity is much larger with $\rho_a/\rho_c = 5.8$ at room temperature, and the initial slope is indicative of a nonmetallic behavior. Qualitatively, these results are in agreement with the band-structure calculations of Raju *et al.*,⁶ who found that the conductivity should primarily take place along the Cr chains (the *c* axis), and very little conduc-

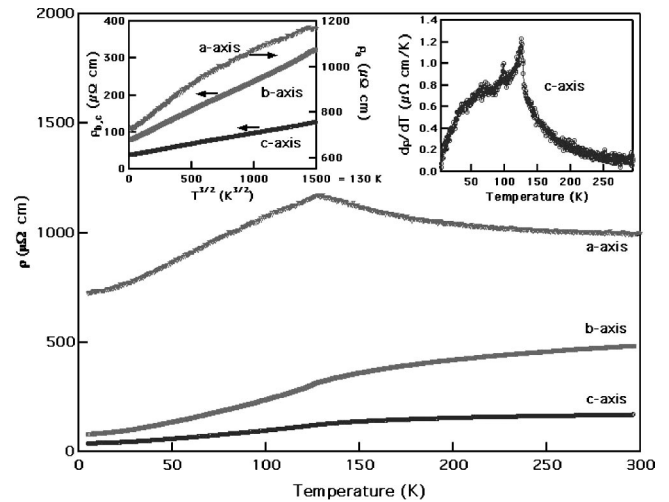
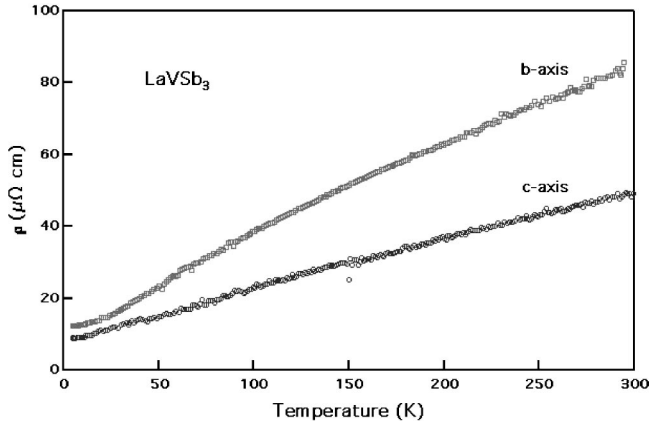
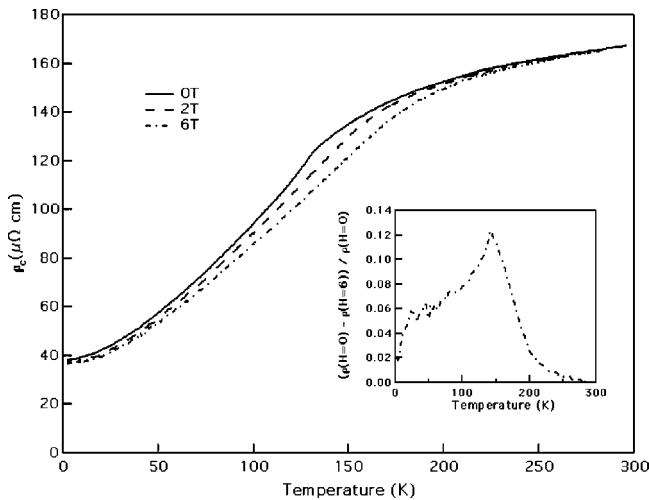
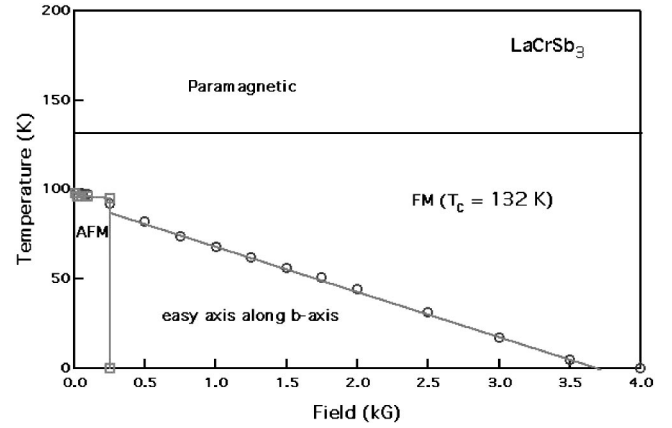


FIG. 7. Resistivity vs temperature of LaCrSb₃. The *a* axis has the largest resistivity, and the *c* axis has the lowest. The inset in the upper right shows $d\rho_c/dT$ with the predicted Fisher Langer-type anomaly, and the inset in the upper left shows the $T^{3/2}$ behavior, typical of a FM.

FIG. 8. In-plane resistivity vs temperature of LaVSb₃.

tivity should be found between the planes (the a axis). The in-plane resistivity for LaVSb₃ is shown in Fig. 8, which shows that this material is metallic down to 5 K, and there is no evidence of any transitions.

All three axes of LaCrSb₃ exhibit evidence of the ferromagnetic transition with a kink in the resistivity at $T_C = 131$ K for each crystallographic orientation. The peak in $d\rho_c/dT$ at the FM transition (the upper right inset in Fig. 7) is attributed to a Fisher-Langer-type anomaly,¹⁷ which is the result of the loss of spin scattering below the Curie point. The ferromagnetic transition is also accompanied with a change in the sign of $d\rho_a/dT$. For $T > T_C$, the in-plane resistivity linearly decreases, while, below T_C , the resistivity decreases as $T^{3/2}$ (upper left inset to Fig. 7). This is an unexpected result because one typically finds the resistivity to decrease as T^2 . However, $T^{3/2}$ behavior is often observed in ferromagnetic systems, in which the scattering length is reduced from an ideal system.¹⁸ The magnetoresistance up to 60 kG is seen in Fig. 9. The greatest change in the resistivity is found near T_C as the Curie temperature is washed out with a large magnetic field. The inset to Fig. 9 shows that the differential magnetoresistance at 60 kG is 12%.

FIG. 9. b -axis magnetoresistivity of LaCrSb₃. The inset shows $[\rho(H=0) - \rho(H=60 \text{ kG})] / \rho(H=0)$ with a peak at T_C .FIG. 10. Phase diagram for the four various magnetic-field- and temperature-dependent regions of LaCrSb₃. The squares show the AFM state as determined by the b -axis magnetization. The circles are data obtained by the c -axis magnetization, and represent T^* . For large temperatures and magnetic fields, the system is FM, and the easy axis is within the plane and oriented in the direction of the magnetic field.

Note the absence of any visible anomaly in the resistivity plots (Fig. 7, both ρ vs T and ρ vs $T^{3/2}$) corresponding to the 98-K AFM transition. This suggests that the spin scattering does not change, and the AFM transition involves a realignment of the ordered moments. This is also consistent with the lack of any evidence for a structural transition in both polycrystalline neutron-diffraction data of Raju *et al.*⁶ and thermal expansion results of Leonard and co-workers,^{4,5} because one would expect a structural transition to have an effect on the scattering length, and therefore a change in the resistivity. In fact, to our knowledge, there is also no evidence of this AFM state in any polycrystalline samples, neither in the low-field magnetization data nor in the neutron-diffraction data reported by Raju *et al.*⁶ Our own polycrystalline samples show a decrease in the magnetization, but the behavior looks very similar to that found at 1 kG, and so it is indistinguishable from the transition at T^* . This is most likely due to a broadening of the AFM transition due to the disorder found in polycrystalline samples. This AFM transition, therefore, can only be observed and investigated using high-quality single crystals. Single-crystal neutron, diffraction measurements are in progress, and will be very useful in understanding the spin alignment.

IV. DISCUSSION

The results discussed above indicate that there are several regions of interest in LaCrSb₃ as the temperature and magnetic field are varied. These results are collected and presented in a temperature vs magnetic-field phase diagram in Fig. 10. For $H=0$ G, there are three regions of interest: a paramagnetic state for $T > T_C = 132$ K, a small FM region for $T_C > T > T_N = 98$ K, and an AFM ground state for $T < 98$ K. As a magnetic field is applied, the AFM state quickly disappears, and the system remains FM below

132 K. In addition, for $H < 3.71$ kG, there is a temperature, T^* , below which the easy axis of magnetization is oriented along the b axis, and the inherent 3D anisotropy of the system is evident. These regions will be discussed in more detail.

Because all of the previous magnetization data were reported on polycrystalline samples, it is useful to compare the results with the single-crystal data. Qualitatively, the two agree with each other, in that they both exhibit a Curie-Weiss behavior at high temperatures, and they both show evidence of a FM transition. The value of T_C was debated within the literature. Both Hartjes *et al.*³ and Raju *et al.*⁶ prepared their samples by a solid-state reaction in vacuum-sealed quartz tubes. They both found a Curie temperature of 125 K, which agrees, within experimental error, with our value for single crystals of $T_C = 132$ K. Leonard *et al.*, who prepared samples using an arc melter, reported a much larger value of $T_C = 144$ K.^{4,5} In order to investigate these differences, and the importance of the sample preparation method, we investigated the Curie temperature on our own arc-melted polycrystalline samples. We used a very similar method to that of Leonard *et al.*,⁴ which involved additional melting of the sample and adding about 10% excess Sb in order to account for its loss during melting. Our polycrystalline samples had a Curie temperature of $T_C = 140$ K (data not shown). These results suggest that a large Curie temperature is a property of arc melting.

The AFM state observed at low temperatures and low applied magnetic fields is an unexpected result, because no indication of this behavior was found in previous studies of this system. The fact that the AFM transition is not observed in zero-field resistivity measurements shows that this AFM state does not lower the electron-spin scattering, which implies that the spins simply realign in another configuration. The easy axis of the AFM state is along the Cr chains (the c axis), while it is perpendicular to the chains (the b axis) in the ferromagnetic state. This observation implies that the spins are always aligned within the b - c plane, but undergo a reorientation within the plane as the field is applied or the temperature is raised. The exact nature of this AFM state is still unknown and further investigation is required.

The downturn which is seen in M_c appears to be an inherent property of the material, due to the fact that it has also been observed (though not explained) in polycrystalline

samples.^{4,5} It appears that the crystalline anisotropy favors spin alignment along the b axis, but there is a potential energy minimum along the c axis which is only slightly favored at low temperatures and low fields. It is possible that this downturn is a remnant of the AFM ground state resulting in a canting of the spins off from the Cr chains. One can rewrite Eq. (1), which relates the temperature at which this downturn occurs, in terms of energies in order to determine the relevant energy scales,

$$8.1 \text{ meV} = k_B T_D + 90.3(2g\mu_B H_D), \quad (2)$$

where g has a free-electron value of 2, and the term in parentheses is the Zeeman energy due to the magnetic field. One finds a small energy scale of 8.1 meV, which is not surprising due to the small magnetic field which is required to destroy the anisotropy within the plane. It is also equivalent to a temperature of 94 K, which is equal (within experimental error) to T_N .

V. CONCLUSION

LaCrSb₃ is an itinerant FM with large anisotropy below T_C . The paramagnetic Curie constant is serendipitously close to that which is expected for Cr³⁺, which would indicate a local-moment system. However, the noninteger value of the saturation moment, coupled with the metallic behavior of the system and the loss of an ESR signal above T_C , all support itinerant ferromagnetism. Below T_C a rich phase diagram is discovered and a large anisotropy observed. The resistivity is lowest along the Cr chains, while the easy magnetization axis is found to be perpendicular to the chains, but still within the b - c plane. At large temperatures and magnetic fields, the moments will align within the b - c plane and orient themselves with the direction of the applied magnetic field, so that the anisotropy is lost within the plane. An unexpected, and still unexplained, result is the presence of an AFM state for $H < 250$ G and $T < 98$ K, which is possibly due to phonon interactions with the itinerant spins.

ACKNOWLEDGMENTS

We would especially like to thank Scott McCall and Gang Cao for their very useful discussions, and John Raymaker for his assistance. This work was funded by the In House Research Program at the National High Magnetic Field Laboratory, which was funded by the NSF, Cooperative Agreement No. DMR-9527035.

*Present address: Lawrence Livermore National Laboratory, 7000 East Ave. L-202, Livermore, California 94550

¹M. Ferguson, R. Hushagen, and A. Mar, *J. Alloys Compd.* **249**, 191 (1997).

²M. Brylak and W. Jeitschko, *Z. Naturforsch. B (Chem. Sci.)* **50**, 899 (1995).

³K. Hartjes, W. Jeitschko, and M. Brylak, *J. Magn. Magn. Mater.* **173**, 109 (1997).

⁴M. Leonard, S. Saha, and N. Ali, *J. Appl. Phys.* **85**, 4759 (1999).

⁵M. Leonard, I. Dubenko, and N. Ali, *J. Alloys Compd.* **303-304**, 265 (2000).

⁶N.P. Raju, J.E. Greedan, M.J. Ferguson, and A. Mar, *Chem. Mater.* **10**, 3630 (1998).

⁷In the work of D. D. Jackson, M. E. Torelli, and Z. Fisk, the remaining compounds of $RCrSb_3$ ($R = \text{Ce-Nd, Sm, Gd}$), were investigated, and will be reported in the near future (unpublished).

⁸A.A.B. Kaiser, *J. Magn. Magn. Mater.* **43**, 213 (1984).

⁹J. Coey, M. Viret, and S. von Molnar, *Adv. Phys.* **48**, 167 (1999).

¹⁰G. Jonker, *Physica (Amsterdam)* **22**, 707 (1956).

¹¹P.G. Radaelli, D.E. Cox, M. Marezio, and S.-W. Cheong, *Phys. Rev. B* **55**, 3015 (1997).

¹²G. Cao, S. McCall, J.E. Crow, and R.P. Guertin, *Phys. Rev. Lett.*

- 78**, 1751 (1997).
- ¹³E. König, *Magnetic Properties of Coordination and Organometallic Transition Metal Compounds* (Springer-Verlag, Berlin, 1966).
- ¹⁴H. Martinho, C. Rettori, and S. Oseroff (unpublished).
- ¹⁵C. Kittel, *Introduction to Solid State Physics*, 7th ed. (Wiley, New York, 1996).
- ¹⁶E. Granado, J. Lynn, D. D. Jackson, and Z. Fisk (unpublished).
- ¹⁷M. Fisher and J. Langer, *Phys. Rev. Lett.* **20**, 665 (1968).
- ¹⁸N. River and A. Mensah, *Physica B* **91**, 85 (1977).